



Synthesis of protein tyrosine phosphatase 1B inhibitors: Model validation and docking studies

Anil K. Saxena*, Gyanendra Pandey, Swati Gupta, Amar Bahadur Singh, Arvind K. Srivastava

Central Drug Research Institute, Medicinal and Process Chemistry, Chattar Manzil Palace, Mahatma Gandhi Marg, Lucknow, Uttar Pradesh 226 001, India

ARTICLE INFO

Article history:

Received 6 October 2008

Revised 20 January 2009

Accepted 16 February 2009

Available online 21 February 2009

Keywords:

Protein tyrosine phosphatases 1B

Docking

Sulfamic acid

ABSTRACT

The designed and synthesized 2-(4-methoxyphenyl) ethyl] acetamide derivatives (**3a**, **3b** and **3c**) were evaluated for their PTP1B inhibitory activity where they showed IC₅₀ values 69 μM, 87 μM and 71 μM, respectively. These results correlated well with the docking studies and in vivo screening of the compounds for their antidiabetic activity in SLM and STZ models.

© 2009 Elsevier Ltd. All rights reserved.

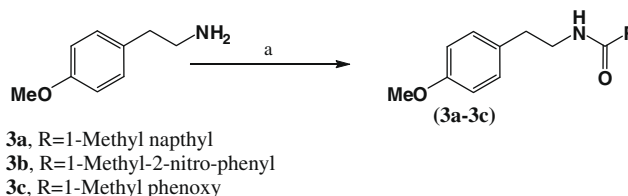
Protein tyrosine phosphatase 1B (PTP-1B) has emerged as a new drug target for the treatment of diabetes and obesity. Protein tyrosine phosphatases (PTPs) constitute a growing family (>90 members) of receptor-like and cytoplasmic signal transducing enzymes.^{1–4} These enzymes are classified on the basis of their cellular localization and are characterized by their common 230 to 280 amino acid catalytic domain termed as PTP signature motif.^{5,6} Several PTPs viz PTP-1B, leukocyte antigen related tyrosine phosphatase (LAR), SH2 domain containing phosphotyrosine phosphatase, PTP α and PTP ϵ are capable of dephosphorylating the tyrosine residues^{7,8} of the insulin receptor, and thereby attenuate the tyrosine kinase activity. The phosphorylation (by protein tyrosine kinases) and dephosphorylation (by PTPs) of tyrosine residues in proteins is recognized as an important cellular regulatory mechanism and many cellular functions could be artificially manipulated exogenously by controlling the activities of these kinases and phosphatases.⁹

The disruption of the above process is at the root of a variety of disease states including cancer, inflammation and diabetes.^{10–14} Studies independently generated by two laboratories, with PTP-1B knockout mice, have demonstrated that the targeted disruption of the PTP-1B gene in mice resulted in enhanced insulin sensitivity and decreased susceptibility to diet-induced obesity.^{15,16} Thus, PTP-1B is considered as an attractive therapeutic target for type-II diabetes as well as for obesity. It may thus provide a new therapeutic option to patients with at-risk obesity or type-II diabetes.

Several three dimensional quantitative structure-activity relationship (3D-QSAR) studies on the PTP-1B have been reported.^{17–21}

As a part of our ongoing programme for targeting PTP-1B in search of potential antidiabetic compounds, we developed 3D-QSAR model on the peptidomimetic competitive inhibitors of PTP-1B.²¹ These studies not only provided insights into the steric, electrostatic, hydrophobic, and hydrogen bonding properties and other structural features influencing the PTP-1B inhibitory activity but also helped to gain an insight about the effect of different conformer based alignments on the quality (in terms of leave one out cross validation, q^2 ; cross validation, r^2 , root mean square error, RMSE) and predictiveness (in terms of r^2_{pred}) of the model. In order to assess or validate the quality of the derived 3D-QSAR model²¹ and to gain new lead molecules, the synthesis and in vitro PTP-1B inhibitory activity of some *N*-[2-(4-Methoxyphenyl)ethyl]-acetamide derivatives which were predicted to show ~75% inhibition at 100 μM along with their docking studies and in vivo antidiabetic activity are reported in this Letter.

The general route for the synthesis of *N*-[2-(4-methoxyphenyl)ethyl] acetamide derivatives is outlined in Scheme 1. Appropriately

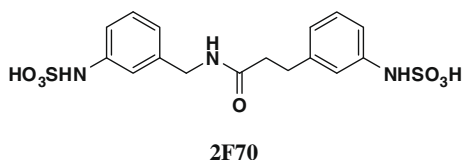


Scheme 1. Reagent and conditions: (a) RCO₂H, DIC, dry DCM, rt.

* Corresponding author. Tel.: +91 522 2612411 18; fax: +91 522 2623405.
E-mail address: anilsak@gmail.com (A.K. Saxena).

substituted carboxylic acids were condensed with the 4-methoxyphenethylamine in the presence of diisopropyl carboximide (DIC) in dry dichloromethane (DCM) to yield the required substituted acetamide.^{27,28}

As vanadate is a non-selective inhibitor of PTPs, and studies have shown that treatment with vanadate can normalize blood glucose level in diabetics,²² the PTP-1B inhibitory activity of *N*-[2-(4-methoxyphenyl)ethyl]-acetamide derivatives was measured at graded doses taking peroxovanadate as a control and the results are summarized in Table 1. The effect of the test compounds on protein tyrosine phosphatase was studied by pre-incubating PTP-1B at the appropriate doses of the test chemicals in the reaction system for 10 min and the residual protein tyrosine phosphatase activity was determined according to the method of Goldstein et al.²³ The activity of PTPase was evaluated using *p*-nitrophenyl-phosphate (PNPP) as the substrate.²⁹



In order to get novel NCEs and to validate our earlier derived best CoMFA model,²¹ three *N*-[2-(4-methoxyphenyl)ethyl]acetamide derivatives (**3a–c**), with considerably high predicted activity 1.33, 0.950 and 0.81 in term of legit transformation of percentage inhibition were designed. These molecules were synthesized and evaluated for their in vitro PTP-1B inhibitory as well as in vivo antidiabetic activities where these compounds **3a**, **3b** and **3c** showed high PTP-1B inhibitory activity 76.9% ($IC_{50} = 69 \mu\text{M}$), 62.5% ($IC_{50} = 87 \mu\text{M}$) and 68.2% ($IC_{50} = 71 \mu\text{M}$) respectively (Table 1).

Since the predicted activity for these compounds cannot be compared in absolute terms with the observed activity due to the difference in the screening model, hence the relative order of the activity was compared. The observed in vitro PTP-1B inhibitory activities of these three new compounds were nearly comparable to their predicted activities by the 3D-QSAR model. The three compounds (**3a**, **3b**, and **3c**) were predicted as **3a** > **3b** > **3c** whereas observed in vitro PTP-1B inhibitory activities of these compounds were in the order **3a** > **3c** > **3b**.

It is evident that the compound **3a**, which was predicted *in-silico* to be the most active, has been observed to be the most active ($IC_{50} = 69 \mu\text{M}$). However, the compound **3b**, predicted to be the next to the most active, was found to be the least active of the three compounds. Nevertheless, all the three compounds **3a**, **3b**, and **3c** showed higher activity than the standard drug (Peroxovanadate, $IC_{50} = 94.6 \mu\text{M}$) in our test model.

In order to gain more insight into the binding mode of these compounds with the enzyme of known X-ray structure, the docking studies were carried out using Genetic Optimisation for Ligand Docking (GOLD) version 2.2 on windows based PC.²⁴ The reported

crystal structure of PTP-1B with co-crystal of sulfamic acids derivative from Protein Data Bank (PDB) ID 2F70,²⁵ with resolution 2.12 Å was downloaded for the present docking study because of the similarity in the structure of 2F70 with amides **3a**, **3b** and **3c**. The docked poses were scored using GOLD score. Initially the protein was considered without ligand and water molecule for the purpose of docking studies. The Protein-ligand complex of PTP-1B (PDB-2F70) was minimised up to a gradient of 0.01 kcal/(mol) and hydrogen were added using the CHARMm force field, available in the software discovery studio 2.0.²⁶ The minimised structure was used for further docking analysis. On finishing point of docking process the resulting conformation poses of *N*-[2-(4-methoxyphenyl)ethyl]acetamide derivatives in the binding sites of PTP-1B were considered. Detailed binding pattern of inhibitor **3a** exhibiting the lowest IC_{50} value is shown in Figure 1. It is interesting to note that the compound **3a** takes the same pose as the sulfamic acid (reference ligand) and also goes into the same active site of PTP-1B. The oxygen of 4-methoxyphenyl group of **3a** shows hydrogen bonding interaction with the $-\text{NH}_2$ of Arg221 similar to the hydrogen bonding interaction of carbonyl of reference ligand with Arg221. The $-\text{NH}$ group of compound **3a** also shows hydrogen bond interaction with water molecule similar to $-\text{NH}$ in the sulfamic acid. However unlike the sulfamic acid, it does not show close interactions with the active site amino acids Ser216, Ala217, Gly220 and Ile219 and with secondary binding site residues of PTP-1B (Arg24, Arg254, Gln262). It has gold score value of 50.66.

The docking studies of the compound **3b** which was lesser active than **3a** and **3c**, show that **3b** does not bind so well with catalytic binding site and shows only one hydrogen bonding interactions with Ile219. It has lower GOLD score value of 45.19 (Fig. 2), however it fits the secondary binding site of PTP-1B very well. The $-\text{NH}$ of the compound **3b** shows hydrogen bonding interaction with the carbonyl group of Gln262 in the same manner as shown by the $-\text{NH}$ in the reference ligand. The nitro group of the compound **3b** shows interaction with Arg24 by hydrogen bonding. Moreover in these interactions the phenyl group of compound **3b** also showed close interaction with Ile219 which is the key residue of catalytic site.

On the other hand the compound **3c** with moderate activity shows no interactions in the catalytic and non catalytic sites but interacts only with one water molecule with the gold score value of 49.85 (Fig. not shown). These studies suggested the activity order of these compounds as **3a** > **3c** > **3b** similar to the results in vitro studies. Hence these three compounds were further evaluated for their antidiabetic activities in the in vivo rodent model viz. sucrose loaded rat model (SLM) and in streptozotocin-induced diabetic rat (STZ) model essentially according to the recently reported procedure from our laboratory.³⁰ The compounds **3a**, **3b** and **3c** showed 25.1%, 19.8% and 24.6% sugar lowering effect in the SLM model (Fig. 3) and 21.4%, 17.5% and 20.6% sugar lowering effect in the streptozotocin-induced diabetic rats (Fig. 4), respectively at a dose of 100 mg/kg against the standard drug metformin (30.2% in SLM and 27.6% in STZ model) (Table 1). It is interesting

Table 1
In vitro PTP-1B enzyme inhibitory and in vivo antihyperglycemic activity in SLM and STZ model for compound **3a–c**

Compounds	% Inhibition at 100 μM		IC_{50} (μM)	Anti- hyperglycemic activity (%) at 100 μM	
	Observed	Predicted ^a		SLM	STZ
3a	76.9	95.5	69 (± 0.20)	25.1	24.1
3b	62.5	90.2	87 (± 0.49)	19.8	17.5
3c	68.2	85.0	74 (± 0.30)	24.6	20.6
Peroxovanadate	56	—	94.6 (± 0.40)	—	—
Metformin	—	—	—	27.2	23.9

^a Predicted from the 3D QSAR model.

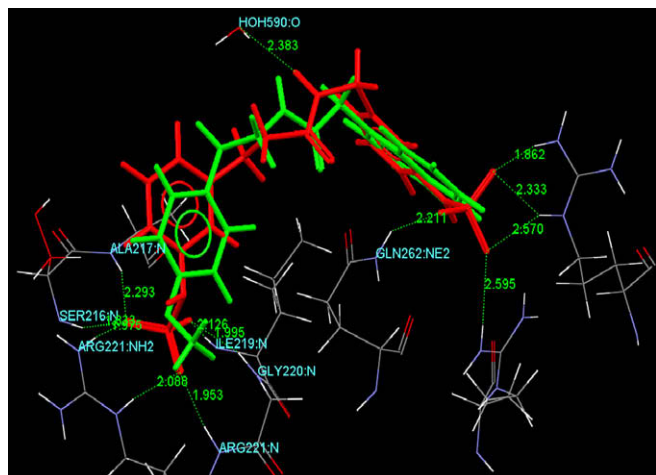


Figure 1. Pose attained by the **3a** (green) and the control ligand (red) in the active site of the PTP1B (PDB ID 2F70).

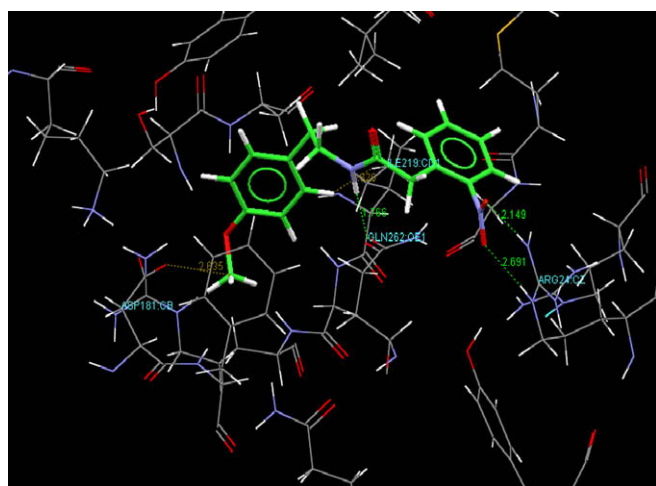


Figure 2. Interaction of the **3b** (green) with the amino acids in the active site of PTP-1B (PDB ID 2F70).

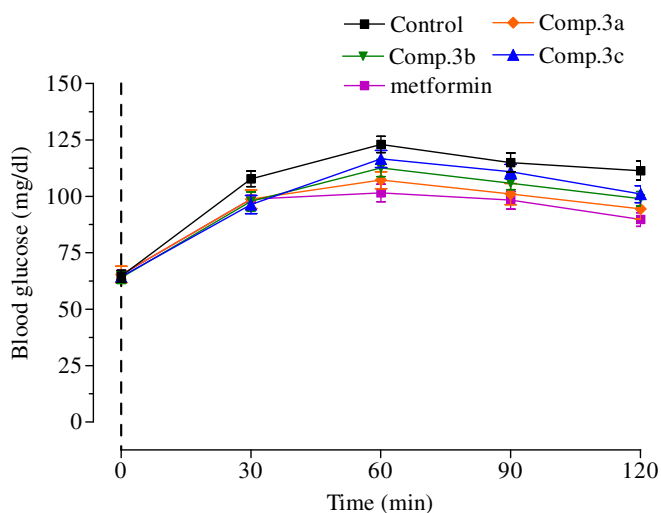


Figure 3. Blood glucose levels in sucrose loaded (SLM) rats before, and up to 2 h after administration of vehicle, compound **3a**, **3b**, **3c** and metformin.

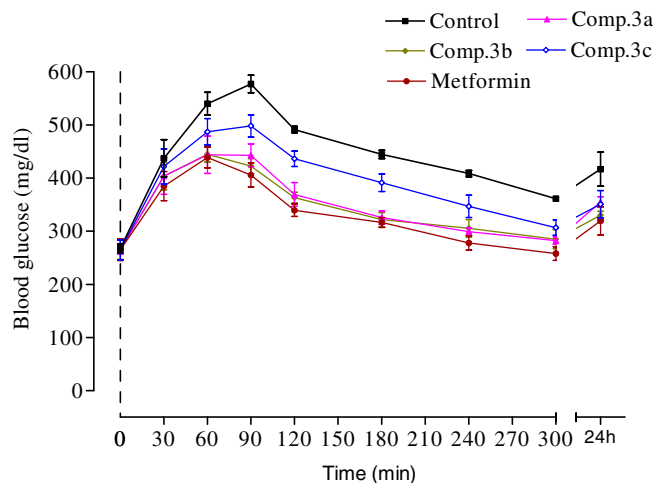


Figure 4. Blood glucose levels in STZ-induced diabetic rats before, and up to 24 h after administration of vehicle, compound **3a**, **3b**, **3c** and metformin.

to note that the in vivo activity of all the three compounds in both the models was also in the same order **3a** > **3c** > **3b** as found in vitro and in docking studies.

It is pertinent to note that the three compounds **3a**, **3b** and **3c** which were predicted to show >75% PTP-1B inhibition at 100 μ M dose by our 3D QSAR model did show high activity but the order of activity predicted to be **3a** > **3b** > **3c** differed and was found to be **3a** > **3c** > **3b**. It may be due to the consideration of single point observation data that too at high fixed molar concentration (100 μ M) because the observed order of activity corresponded well with the IC₅₀ value data determined for these compounds as well as with the docking results in terms of gold score values and in vivo antidiabetic activity data in both SLM and STZ models. It may be inferred from the docking score results **3a** > **3c** > **3b** that the hydrogen bonding interactions at the active site residues Arg221 (**3a**) has more influence on binding than the interaction with Ile219 (**3b**). The observed activity of **3c** is higher than **3b** and lesser than **3a** suggest that the hydrogen bonding interaction with water molecule provide better binding affinity than the hydrogen bonding interaction with secondary site residue Arg24.

Acknowledgements

Authors are thankful to Messers Z. Ali and A.S. Kushwaha for the technical assistance; SAIF, Lucknow, for providing spectroscopic data and Network project on Diabetes mellitus new drug discovery R&D for the financial supports. One of the authors SG is thankful to ICMR, New Delhi for the award of senior research fellowship.

References and notes

- Neel, B. G.; Tonks, N. K. *Curr. Opin. Cell Biol.* **1997**, *9*, 193–204.
- Denu, J. M.; Stuckey, J. A.; Saper, M. A.; Dixon, J. E. *Cell.* **1996**, *87*, 361–364.
- Jia, Z. *Biochem. Cell Biol.* **1997**, *75*, 17–26.
- Zhang, Z. Y. *Crit. Rev. Biochem. Mol. Biol.* **1998**, *33*, 1–5.
- Lander, E. S. et al *Nature* **2001**, *409*, 860–921.
- Venter, J. C. et al *Science* **2001**, *291*, 1304–1351.
- Evans, J. L.; Jallal, B. *Exp. Opin. Invest. Drugs.* **1999**, *8*, 139–160.
- Burke, T. R.; Zhang, Z. Y., Jr *Biopolymers (Pept. Sci.)* **1998**, *47*, 225–241.
- Ahn, N. *Chem. Rev.* **2001**, *101*, 2207–2208.
- Bandyopadhyay, D.; Kusari, A.; Kenner, K. A.; Liu, F.; Chernoff, J.; Gustafson, T. A.; Kusari, J. *J. Biol. Chem.* **1997**, *272*, 1639–1645.
- Wang, X. Y.; Bergdahl, K.; Heijbel, A.; Liljebri, C.; Bleasdale, J. E. *Mol. Cell. Endocrinol.* **2001**, *173*, 109–119.
- Jacob, K. K.; Sap, J.; Stanley, F. M. *J. Biol. Chem.* **1998**, *273*, 4800–4809.
- Goldstein, B. J. *J. Cell. Biochem.* **1992**, *48*, 33–42.
- Elchebly, M.; Payette, P.; Michaliszyn, E.; Cromlish, W.; Collins, S.; Loy, A. L.; Normandin, D.; Cheng, A.; Himms-Hagen, J.; Chan, C. C.; Ramachandran, C.;

- Gresser, M. J.; Tremblay, M. L.; Kennedy, B. P. *Science*. **1999**, *283*, 1544–1548.
15. Klamann, L. D.; Boss, O.; Peroni, O. D.; Kim, J. K.; Martino, J. L.; Zabolotny; Moghal, N.; Lubkin, M.; Kim, Y. B.; Sharpe, A. H.; Stricker-Krongrad, A.; Shulman, G. I.; Neel, B. G.; Kahn, B. B. *Mol. Cell Biol.* **2000**, *20*, 5479–5489.
 16. Murthy, V. S.; Kulkarni, V. M. *Bio. Med. Chem.* **2002**, *107*, 2267–2282.
 17. Hu, X.; Stebbins, C. E. *Bio. Med. Chem.* **2005**, *134*, 1101–1109.
 18. Zhou, M.; Ji, M. *Bio. Med. Chem. Lett.* **2005**, *1524*, 5521–5525.
 19. Larsen, S. D.; Barf, T.; Liljebriis, C.; May, P. D.; Ogg, D.; O'Sullivan, T. J.; Palazuk, B. J.; Schostarez, H. J.; Stevens, F. C. *J. Med. Chem.* **2002**, *45*, 598–622.
 20. Sekar, N.; Li, J.; Shechter, Y. *Crit. Rev. Biochem. Mol. Biol.* **1996**, *31*, 339–359.
 21. Pandey, G.; Saxena, A. K. *J. Chem. Info. Model* **2006**, *46*, 2579–2590.
 22. Meyerovitch, J.; Farfel, Z.; Sack, J.; Shechter, Y. *J. Biol. Chem.* **1987**, *262*(14), 6658–6662.
 23. Goldstein, B. J.; Bittner-Kowalczyk, A.; White, M. F.; Harbeck, M. *J. Biol. Chem.* **2000**, *275*, 4283–4289.
 24. GOLD; Version 2.2; Cambridge Crystallographic Data Centre: Cambridge, UK.
 25. Klopfenstein, S. R.; Evdokimov, A. G.; Colson, A. O.; Fairweather, N. T.; Neuman, J. J.; Maier, M. B.; Downs, T. R.; Kasibhatla, B.; Peters, K. G. *Bio. Med. Chem. Lett.* **2006**, *16*, 1574–1578.
 26. Discovery Studio 2.0, Accelrys Inc., San. Diego, CA, USA.
 27. *Experimental*: Melting points were determined on an electrical heated m.p apparatus. Infrared spectra (IR) were recorded on Perkin-FTIR model PC spectrophotometer with frequency of absorptions reported in wave numbers. MS were recorded on JEOL spectrometer. The NMR spectra were recorded on Bruker DPX 200 MHz spectrometer.
 28. *General procedure*: The general route for the synthesis of *N*-[2-(4-methoxyphenyl)ethyl]-2-naphthalen-1-yl-acetamide (**3a**): The 4-methoxy phenyl amine (0.468 ml, 0.0032 mol) in dry DCM was added to the stirred solution of naphthalen-1-yl-acetic acid (0.600 g, 0.0032 mol) in dry dichloromethane (DCM) and diisopropyl carboximide (DIC) at 0 °C. The reaction mixture was stirred at room temperature for 8 hours. The solvent was evaporated under vacuum, and the residue was triturated with hexane and DCM. The separated DCU was removed by filtration and the filtrate was concentrated give **3a**, which was purified by column chromatography, using chloroform: methanol (98:2) as mobile and silica gel G as stationary phase. Yield: 0.500 g (42%); mp: 120 °C. Anal. Calcd for C₂₁H₂₁NO₂: C, 78.99; H, 6.58; N, 4.38. Found: C, 79.01; H, 7.00; N, 4.40. ¹H NMR (CDCl₃, 200 MHz): δ 2.46–2.53 (t, *J* = 6.6 Hz, 2H), 3.29–3.39 (m, 2H), 3.73 (s, 3H), 3.99 (s, 2H), 5.70 (br s, 1H), 6.54–6.64 (m, 3H), 7.25–7.56 (m, 5H), 7.79–7.92 (m, 3H); IR (KBr): 777, 1247, 1605, 3296; FAB-MS: *m/z* (M+1)⁺ 320; Compounds **3b** and **3c** were synthesized similarly. *N*-[2-(4-Methoxyphenyl)ethyl]-2-(2-nitrophenyl)-acetamide (**3b**): Yield: 0.700 g (50%); mp: 104 °C. Anal. Calcd for C₁₇H₁₈N₂O₄: C, 64.96; H, 5.73; N, 8.91. Found: C, 64.98; H, 5.76; N, 8.93. ¹H NMR (CDCl₃, 200 MHz): δ 2.72–2.76 (t, *J* = 6.80 Hz, 2H), 3.46–3.49 (m, 2H), 3.78 (s, 5H), 6.77–6.81 (d, *J* = 8.6 Hz, 2H), 7.01–7.06 (d, *J* = 8.6 Hz, 2H), 7.44–7.48 (d, *J* = 7.2 Hz 2H), 7.50 (m, 1H), 8.01 (m, 1H); IR (KBr): 713, 1243, 1609, 3298; FAB-MS: *m/z* (M+1)⁺ 315. *N*-[2-(4-Methoxyphenyl) ethyl]-2-phenoxy-acetamide (**3c**): Yield: 61%; mp: 112 °C. Anal. Calcd for C₁₇H₁₉NO₃: C, 71.57; H, 6.66; N, 4.91. Found: C, 71.59; H, 6.69; N, 4.93. ¹H NMR (CDCl₃, 200 MHz): δ 2.01 (br s 1H), 2.77–2.80 (m, 2H), 3.54–3.57 (m, 2H), 3.78 (s, 3H), 4.46 (s, 2H), 6.79–6.87 (m, 4H), 7.02–7.08 (m, 3H), 7.26–7.31 (m, 2H); IR (KBr): 753, 1242, 1655, 3345; FAB-MS: *m/z* (M+1)⁺ 286.
 29. Assay mixture containing 10 mM PNPP in 50 mM HEPES buffer (pH 7.0), with 1 mM EDTA and DTT was made up to 1 ml. The reaction was stopped by the addition of 500 μl of 0.1 N NaOH and absorbance was determined at 410 nm. A molar extinction coefficient of 1.78 × 10⁴ M⁻¹ cm⁻¹ was used to calculate the concentration of *p*-nitrophenolate ions produced in the reaction mixture. The IC₅₀ values were calculated from the % inhibition of the PTPase at five different doses (10, 25, 50, 75 and 100 μM).
 30. Maurya, R.; Akanksha; Jayendra; Singh, A. B.; Srivatava, A. K. *Bio. Med. Chem. Lett.* **2008**, *18*, 6534–6537.